

Article

Real-Time Detection of Nickel Plated Punched Steel Strip Parameters Based on Improved Circle Fitting Algorithm

Binfang Cao ^{1,2}, Jianqi Li ^{2,*}, Yincong Liang ², Xuan Sun ² and Weihao Li ²¹ College of Mathematics and Physics Science, Hunan University of Arts and Science, Changde 415000, China² Hunan Provincial Key Laboratory for Control Technology of Distributed Electric Propulsion Aircraft, Changde 415000, China

* Correspondence: li_jianqi@126.com

Abstract: Nickel-plated punched steel strip is a product obtained by punching holes on the surface of cold-rolled white sheet steel strip and then electrochemical nickel plating. It is necessary to make accurate and fast detection of punching circle parameters, since it is of crucial importance to ensuring the quality of nickel-plated punched steel strips. Accordingly, in this article, an improved circle fitting algorithm of nickel-plated punched steel strip is proposed. Firstly, the least squares fitting is performed to obtain the circle center and radius dataset by iterative algorithm with different values for the initial point positions and intervals. Then, the mean shift algorithm is used to optimize the results after iteration, and the segmented fitted circle centers are all concentrated around the true circle center to obtain the best radius and center coordinates. Finally, comparison experiments with different numbers of circular holes and verification experiments with nickel-plated punched steel strips are carried out. As the results show, the algorithm proposed in this article is more robust than the least squares algorithm in detecting multiple circles and has better real-time performance than the Hough transform. Therefore, it can meet the industrial production needs with high accuracy and real-time requirements, such as nickel-plated punched steel strips.

Keywords: nickel-plated punched steel strip; multi-circle detection; least square method; mean shift



Citation: Cao, B.; Li, J.; Liang, Y.; Sun, X.; Li, W. Real-Time Detection of Nickel Plated Punched Steel Strip Parameters Based on Improved Circle Fitting Algorithm. *Electronics* **2023**, *12*, 1865. <https://doi.org/10.3390/electronics12081865>

Academic Editor: Chiman Kwan

Received: 11 February 2023

Revised: 8 April 2023

Accepted: 12 April 2023

Published: 14 April 2023



Copyright: © 2023 by the authors. Licensee MDPI, Basel, Switzerland. This article is an open access article distributed under the terms and conditions of the Creative Commons Attribution (CC BY) license (<https://creativecommons.org/licenses/by/4.0/>).

1. Introduction

Under the goal of “dual carbon” in the world, countries have reduced demand for fossil fuels. The application of clean energy such as electricity is becoming more and more extensive. Electric vehicles are developing rapidly in this context. High-performance power batteries, which store electricity and provide it to motors, are the core components of electric vehicles. Moreover, the performance of the battery determines the comprehensive performance and range of the electric vehicle. Nickel-plated punched steel strip is currently the key basic material for the preparation of high-performance power battery [1,2]. Nickel-plated punched steel strip is usually used as a battery current collector material, and its manufacturing process includes two parts: punching on the surface of cold rolled white steel strip and plating electrochemical nickel. It has good electrical conductivity and corrosion resistance and high-cost performance, suitable for large-scale continuous production. The punching process in the processing of nickel-plated punched steel strip is the key link in the formation of the product. The perforation hole diameter, horizontal hole distance and vertical hole distance are the key technical indicators of the punching system. Due to various reasons, the punched holes may have defects such as blind holes, uneven steps and continuous holes. The industrial site requires real-time and accurate detection of punching circle parameters so that these defects can be checked in time to ensure product performance and quality.

At present, the site uses manual sampling inspection, but the manual sampling inspection has the problem of low efficiency and easy to miss detection. In addition, manual

sampling is not possible during the production process since perforated steel strips are produced continuously in rolls, resulting in quality defects that cannot be detected in time even if they exist. Therefore, accurate and rapid inspection of punching circle parameters is very important to ensure the quality of nickel-plated punched steel strip.

Given the fact that the manual inspection is labor-intensive and of low efficiency and low accuracy, in recent years, automatic surface inspection using machine vision has been applied [3–8]. Generally, the defect detection based on machine vision could be regarded as a special object detection task.

Currently, the more widely used methods for detecting circle parameters are Hough transform [9–12] and least squares fitting method [13,14]. Among them, the Hough transform detects circle parameters by mapping the image space to the parameter space and accumulating the edge points in the parameter space. However, the detection result is obtained from the parameter calculation of the accumulated values, suffering from the problem of time complexity and space complexity. To overcome these problems, the theoretical properties and application methods of the Hough transform have been improved, such as Marco et al. [15] who present a randomized iterative workflow, which exploits geometrical properties of isophotes in the image to select the most meaningful edge pixels and to classify them in subsets of equal isophote curvature. Barbosa et al. [10] present an improvement on the voting process to detect multiple circles using Hough transform to avoid false positives, and the experiments show that the voting process leads to a more robust detection, reducing the number of false positives and providing a more accurate detection even with large number of circles. Another parameter detection method for circles is the least squares fitting method. Although the conventional least squares circle fitting algorithm has excellent results, it is difficult to meet the accuracy requirements because the punched steel strip image studied in this article has more punched circles and high-accuracy requirements. The mean shift algorithm is a density-based nonparametric clustering algorithm [16–18], which is widely used in image processing and computer vision technology, such as image denoising, image segmentation, motion tracking, etc. In order to solve this problem and to improve the real-time accuracy of circle fitting as the starting point, an improved algorithm for multi-circle fitting of punched steel strips is proposed in this article.

In summary, the main contributions of this article are given as follows.

(1) There are generally 20–30 punching circles on the image of the punched steel strip studied in this article and using Hough transform tends to cause the parameter space of the circle to become larger and the program to run slower [10,15]. In addition, it would make the real-time needs of the system hard to meet. Hence, an improved circle fitting algorithm based on the least squares method is proposed in this article;

(2) Firstly, the least squares fitting is performed to obtain the circle center and radius dataset by iterative algorithm with different values for the initial point positions and intervals. Then, the mean shift algorithm is used to optimize the results after iteration, and the segmented fitted circle centers are all concentrated around the true circle center to obtain the best radius and center coordinates;

(3) Finally, comparison experiments with a different number of circular holes and verification experiments with nickel-plated punched steel strips are carried out. The proposed method has better performance considering the computational accuracy of the parameters and the real-time performance.

The rest of this article is organized as follows. Section 2 presents improved multi-circle fitting algorithm based on the least squares method of punched steel strip. Section 3 describes the experiments and the analysis of results. Finally, Section 4 presents the conclusions of this study.

2. Improved Multi-Circle Fitting Algorithm Based on the Least Squares Method of Punched Steel Strip

The improved circle fitting algorithm proposed in this article is as follows. Firstly, the acquired punched steel strip images are preprocessed, specifically including median filtering, threshold segmentation, morphological erosion and edge extraction. Secondly, the least squares fitting is performed to obtain the circle center and radius datasets by an iterative algorithm with different values for the initial point locations and intervals. Finally, the mean shift algorithm is used to optimize the iterated results, and the segmented fits are focused on the true circle centers to obtain the best radius and center coordinates.

2.1. Circle Detection and Parameter Iteration

Using the concept that any three points in the plane can determine a unique circle, three points are first selected each time. Due to the extremely high accuracy requirements of this experimental object, the remaining points that are not co-linear are also selected at equal intervals to improve the accuracy of circle detection and make the calculation process simpler. This series of pixel points $(X_i, Y_i) i \in (1, 2, 3, \dots, N)$ fall approximately on a circle, then the distance d_i from the point in (X_i, Y_i) to the center of the circle (X_0, Y_0) is described as follows [12,19,20]:

$$d_i^2 = (X_i - X_0)^2 + (Y_i - Y_0)^2 \quad (1)$$

where $(X_i, Y_i) i \in (1, 2, 3, \dots, N)$ is the coordinates of the feature point on the arc. N is the number of feature points participating in the fit. The radius of the circle is assumed as r , the optimization objective function of the error squared is defined as follows

$$S = \sum_{i=1}^N [\sqrt{(X_i - X_0)^2 + (Y_i - Y_0)^2} - r]^2 \quad (2)$$

An improved method to define the error squared while avoiding the square root, while maintaining this optimized objective function characteristic, is given by the following definition

$$E = \sum_{i=1}^N [(X_i - X_0)^2 + (Y_i - Y_0)^2 - r^2] \quad (3)$$

Then, expanding Equation (3)

$$E = \sum_{i=1}^N (X_i^2 - 2X_0X_i + X_0^2 + Y_i^2 - 2Y_0Y_i + Y_0^2 - r^2) \quad (4)$$

Let $B = -2Y_0$, $A = -2X_0$, $C = X_0^2 + Y_0^2 - r^2$, and then bring A , B , C into Equation (4), so we can get Equation (5) as follows:

$$E = \sum_{i=1}^N (X_i^2 + Y_i^2 + AX_i + BY_i + C) \quad (5)$$

According to the principle of least squares, when E takes a very small value, the coordinates of the center of the fitted circle, the fitted value of the radius r is found as follows:

$$X_0 = -\frac{A}{2}, Y_0 = -\frac{B}{2}, r = \frac{1}{2} \sqrt{A^2 + B^2 - 4C} \quad (6)$$

In this article, the iteration is performed by using the values of the iterative variables T and T_b for the initial point position and the fetch interval of the circle fit, respectively.

The specific iterative steps (Algorithm 1) are as follows:

Algorithm 1. Iterative algorithm

Input: T, T_b
 (T is the initial position of the circle fit, and T_b is the interval between the points)
 Output: T_a

1. $T_a = T;$
2. $T_a = T_a + T_b;$
3. If the number of $T_a <$ Maximum number of points;
4. $T_b++;$
5. $T_a = T_a + T_b;$
6. If the number of $T_a <$ 3;
7. $T++;$
8. $T_a = T;$
9. Else T_a performs least squares.

The above iterative algorithm and the least squares method are used to calculate the circular hole parameters of the nickel-plated punched steel strip and obtain the dataset of circle center coordinates and radius, which can effectively eliminate some noise points in the fitting results and improve the robustness of the fitting.

2.2. Mean Shift-Based Parameter Optimization

The centers of the circles fitted by least squares segmentation are concentrated around the true center of the circle. In order to obtain the best radius and center coordinates, the Mean Shift algorithm is used in this article to optimize the results after iteration. The mean shift algorithm is a density-based nonparametric clustering algorithm [16,17], which is calculated by assuming that the dataset containing n objects follows different probability density distributions. First, the initial values of the parameters are determined, including the number of cluster sets and the radius of the high-dimensional region h . Then, for any point x in the cluster set space, the mean shift vector $M(x)$ is derived, defined as follows:

$$M_h(x) = 1/k \sum_{x_i \in S_k} (x_i - x) \quad (7)$$

where S_k is a high-dimensional region of radius h , the set $S_k(x_i)$ of x_i points satisfying the following relation:

$$S_k(x_i) = \{x_i : (x_i - x)(x_i - x) < h^2\} \quad (8)$$

k indicates that in these samples, k landing points fall in the region. x is the starting point. After that, for each point x in the cluster set space is updated and its mean shift vector is calculated as follows:

$$x := x + M(x) \quad (9)$$

If the value of $M(x)$ is less than a threshold or the number of iterations reaches a certain threshold, the algorithm is stopped. Otherwise, the region is updated using the center of mass of the mean shift vector as the high-dimensional region round point, and the above operation is continued.

2.3. Our Proposed Improved Circle Fitting Algorithm

The specific process of the improved circle fitting algorithm proposed in this article is as follows. Firstly, the acquired punched steel strip images are pre-processed, specifically including median filtering, threshold segmentation, morphological erosion and edge extraction. Then, the least-squares fitting is performed to obtain the circle center and radius dataset by taking different values for the initial point positions and intervals through an iterative algorithm. Finally, the mean shift algorithm is used to optimize the fitted set of circular hole parameters to obtain the circle center and radius parameters. The detailed steps of the algorithm proposed in this article are as shown below.

Step 1: Image preprocessing.

First, the acquired image is smoothed by median filtering, and the Otsu threshold segmentation algorithm is used to segment the target circle from the image background of the punched steel strip image, and the black part is obtained after binarization. Then, the incomplete circle in the boundary area is rejected, and the judgment criterion is to scan the incomplete circle in the boundary area with a circle composed of the calibrated circle center and radius, and get the number of pixels of the scanned circle and the boundary area circle. If the number of overlapping target pixel points is greater than 0.8 of the average circle pixel points, it is judged to be a complete circle, and its circle center coordinates and aperture parameters are recorded; otherwise, it is discarded. See the reference [21] for more image preprocessing details.

Step 2: Using Algorithm 1 in Section 2.1, the circle center parameters and radius of the points taken out at different initial points and different intervals are calculated. After extracting the contour points using contours, each subset C_i obtained is saved, and then the number of segment points count is set, and each point is least-squares fitted once according to count, and finally the group of N center points of a circle $\{X_1, X_2, \dots, X_n\}$ is obtained.

Step 3: Using the mean shift algorithm to find the optimal circle center coordinates and radius for the fitted set of circle hole parameters.

- The center of mass of the initial group of centroid points is found, marked as *oldCenter*, and the value of the mean variable in the mean shift algorithm is replaced by the value of the center of mass, which is calculated as follows, with the *oldCenter* as the center of the scan set according to the scan radius R set in advance parameters.

$$oldCenter = \sum X_i / N \quad (10)$$

- To find the center of mass of the group of circle centers in the scan area, update the scan center and assign its value to the variable *newCenter*.
- The accuracy *Ess* is first calculated from the *oldCenter* and *newCenter*, and the expression is as follows:

$$Ess = D(oldCenter, newCenter) \quad (11)$$

where D denotes the calculation of the Euclidean distance expression, calculated as follows:

$$D = \sqrt{(A_x - B_x)^2 + (A_y - B_y)^2} \quad (12)$$

where $(A_x, A_y), (B_x, B_y)$ represent *oldCenter, newCenter* coordinates, respectively. If the accuracy does not meet the initial set threshold, continue to execute Step 4, update the value of *newCenter, oldCenter* with the initial center of mass value remains unchanged, until the initial set accuracy *Ess* is met.

- Calculating the Euclidean distance between the final center of mass and the other circle centers within the scan radius, finding the circle center with the smallest distance, and drawing the circle corresponding to that center, thus deriving the group of N center points $\{X_1, X_2, \dots, X_n\}$ of a certain circle of the fitted final circle centers.

Step 4: Taking the result of the merit search as the center and radius of the current circle.

Step 5: Skipping to step 2, continuing to fit the above algorithm to the group of center points of other circles, finally arriving at all the best center points on the punched steel strip, and drawing all the circles corresponding to the center of the circle.

3. Experiments and Analysis of Results

3.1. Experimental Setups

The punched steel strip surface defect detection system is shown in Figure 1. In order to avoid the impact of surface chromatic aberration and contamination of the material to be tested, the project uses the backlighting method to irradiate the object to be tested. The

working process of the system is as follows. Firstly, punching a section of steel strip, when the Programmable Logic Controller (PLC) of the control unit (Siemens S7-226) detects the winding stop signal (external photoelectric switch signal), it starts the image acquisition of the steel strip on the fixed plane. Then, when detecting the punching stop signal (external photoelectric switch signal), it starts the inverter to drive the winding motor for the winding operation, the whole process continuously cycles the winding operation and punching. Finally, the image samples collected are saved and the measured values of the steel strip punching process are calculated and displayed in the software system. The pixel equivalents are $X = 0.003826$, $Y = 0.003826$.



Figure 1. The diagram of hardware system.

3.2. Multi-Circle Parameter Measurement and Performance Comparison

The real-time operation and robustness of the algorithms in this article for multi-circle detection are first tested. MATLAB 2018 (a) programming was used to implement the algorithm of this article, the least squares algorithm and the Hough transform algorithm for multi-circle detection, respectively. A PC with a 2.6 GHZ Intel(R) Core(TM) i7-6498DU CPU and 4 GB RAM was used with a Windows 10 Home Edition platform.

In this article, five images of nickel-plated punched steel strip with different numbers of round holes are used, as shown in Figure 2, where the images with different numbers of round holes are intercepted from the original images of nickel-plated punched steel strip, which can ensure that the parameters of round holes are basically the same.

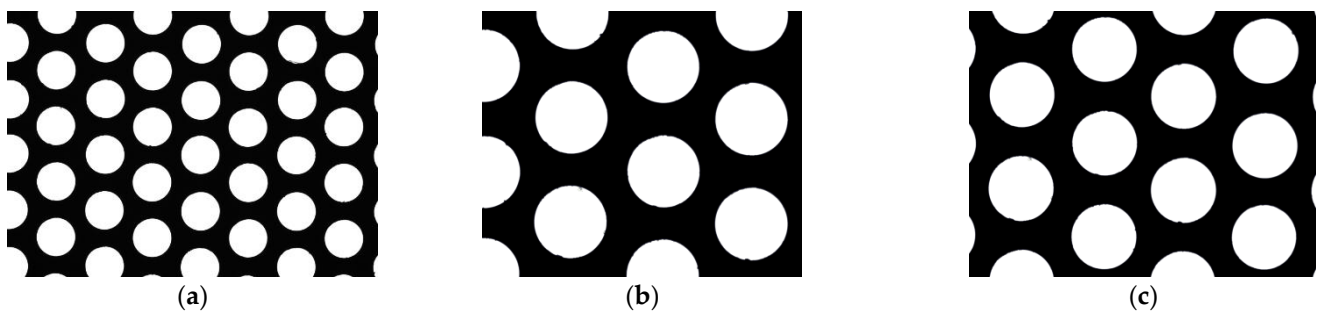


Figure 2. Cont.

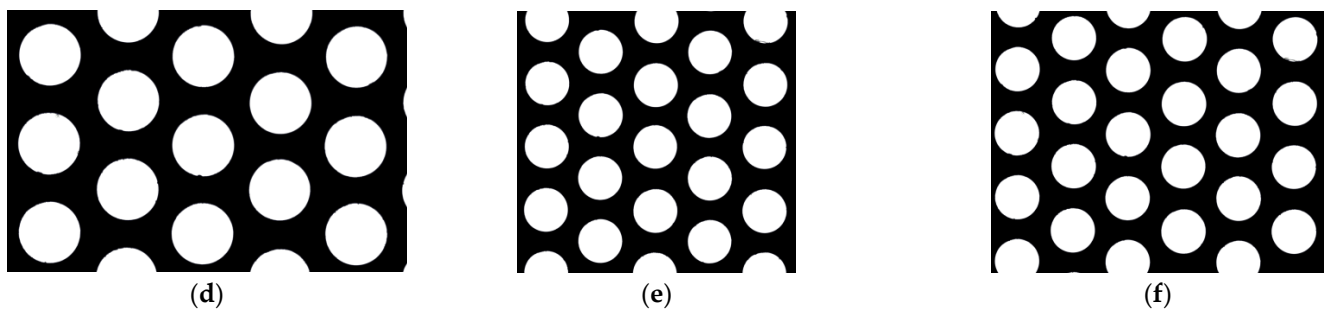


Figure 2. Experimental images of different number of punched circles. (a) The original image of nickel-plated punched steel strip. (b) The image of 6 round holes. (c) The image of 10 round holes. (d) The image of 15 round holes. (e) The image of 17 round holes. (f) The image of 21 round holes.

Firstly, the images of five types of nickel-plated punched steel strip with different numbers of round holes were preprocessed, including median filtering, threshold segmentation, morphological erosion and edge extraction. The median filtering is used to filter out external noise from the factory-acquired image, using a 3×3 template and the Otsu threshold segmentation algorithm is used to segment the target circle from the image background of the punched steel strip image, and the black part is obtained after binarization. Then, disc structure elements are selected and morphological corrosion is used to extract the boundary, where the strel parameter is set to $se1 = strel('disk', 3)$.

Then, the proposed method, the least squares algorithm and the Hough transform algorithm were used for multiple circle detection. The time required for multi-circle inspection using the three methods is given in Table 1, and the diameter of the holes obtained using the three different algorithms is given in Table 2. The error curves of the diameter of the holes calculated by the three methods are given in Figure 3, where the absolute error is defined as follows:

$$\text{Absolute error} = |\text{Calculated value} - \text{Standard value}| \tag{13}$$

where the standard value of hole diameter is 1.5135 mm. Because there is no standard value for the circular center parameter of the circular hole, no comparison is made in this article.

Table 1. The time to detect multiple circles by different algorithms.

Methods	Images				
	Figure 2b	Figure 2c	Figure 2d	Figure 2e	Figure 2f
Least squares method	1.3175	1.8281	2.5156	2.7344	3.2656
Hough transform	2.6563	3.1250	4.3813	5.0344	5.5781
Proposed method	2.0313	2.2813	2.5313	2.6875	2.8281

Table 2. The diameter of the circular hole obtained by different algorithms (mm) lists look like this.

Methods	Images				
	Figure 2b	Figure 2c	Figure 2d	Figure 2e	Figure 2f
Least squares method	1.5184	1.5187	1.5169	1.5163	1.5167
Hough transform	1.5151	1.5143	1.5145	1.5155	1.5147
Proposed method	1.5140	1.5141	1.5140	1.5141	1.5143

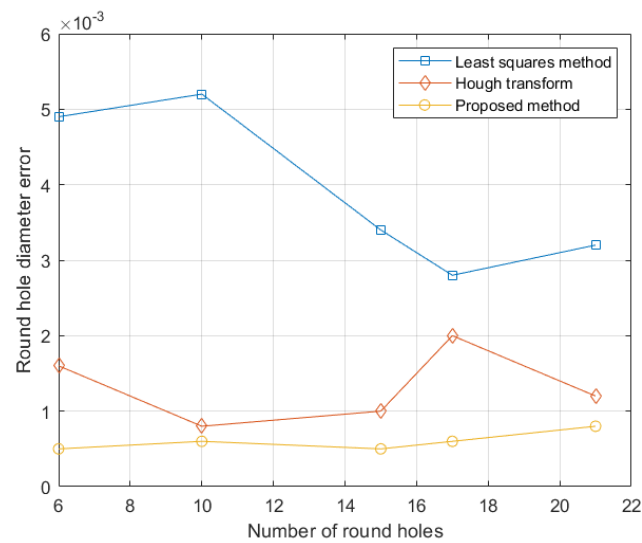


Figure 3. The error curve of circular hole diameter for different number of punched circles in Figure 2.

As can be seen from Table 1, with the increase in the number of circular holes, the running time of all three algorithms increases, but the time increase in the proposed method is smaller. In addition, the real-time performance for multi-circle detection is significantly better than that of the least squares and Hough transform methods. As can be seen from Table 2 and Figure 3, the detection accuracy of our proposed algorithm for circular hole parameters is higher than that of the other two methods. The above results show that the proposed method has high real-time performance and robustness. The reason for this is that the method in this article carries out several iterations based on the good real-time performance of the least squares method, and then the mean shift algorithm is used to optimize the fitted set of circular hole parameters and obtain the center and radius parameters. It not only retains the advantages of the least squares algorithm in terms of good real-time performance, but also improves the disadvantages of the poor robustness of the least squares.

3.3. Parameter Measurement and Result Analysis of 145 Type of Punched Steel Strip

In this article, a nickel-plated punched steel strip of type $180 \times 145.6 \times 0.09$ -B (145) is tested. The images of the nickel-plated punched steel strip are shown in Figure 4a, then the median filtering is used to filter out external noise from the factory-acquired image, using a 3×3 template.

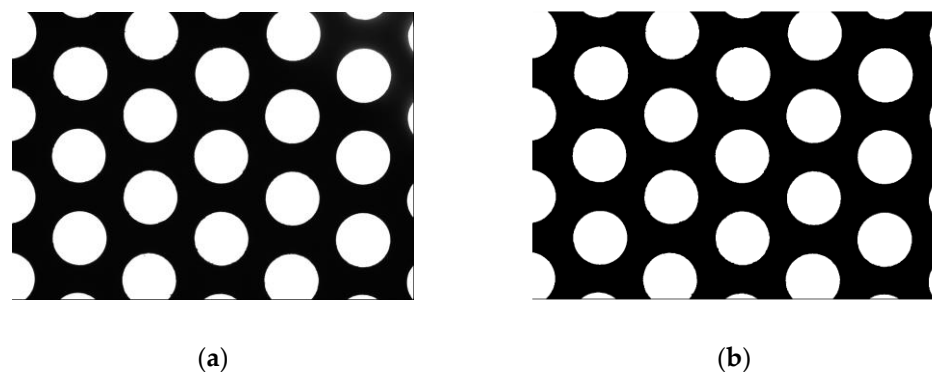


Figure 4. Cont.

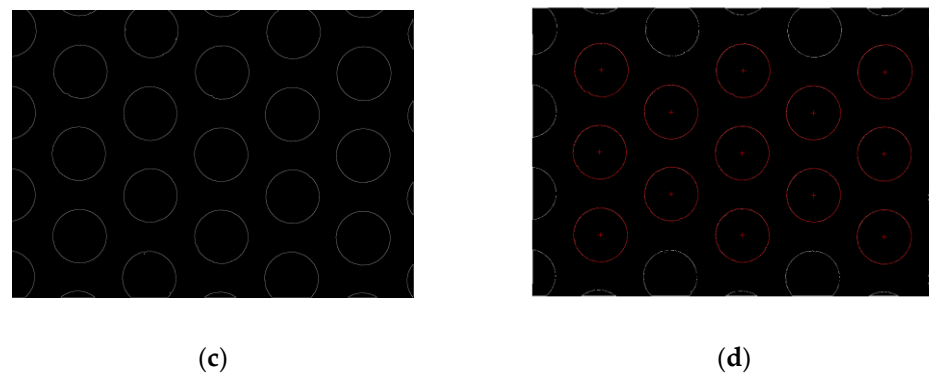


Figure 4. The fitting effect of 145 type of punched steel stripe. (a) The image of 145 type of punched steel stripe. (b) The image of 145 type of punched steel strip after global threshold processing. (c) The image after using morphological edge detection. (d) Fitting results after using least squares method.

Figure 4b shows the image after achieving the target circle segmentation of the perforated steel strip image using the Otsu thresholding segmentation algorithm. Figure 4c shows the image after using morphological edge detection, where the strel parameter is set to $se1 = strel('disk', 3)$. Figure 4d shows the fitting results using proposed method, where $T_a = 100, T_b = 30, T = 120$, the red lines are the fitted circles. It can be clearly seen that the contour of the fitted circle forms a basic match with the round hole of the steel strip, and the center of the circle is marked by the red “+”.

The hole diameter error curve of punched steel strip of No. 145 is shown in Figure 5, where the standard value of hole diameter is 1.963 mm. As shown in Figure 5, comparison curves are given for calculating the hole diameter errors of 145 type of nickel-plated punched steel stripe by three different methods.

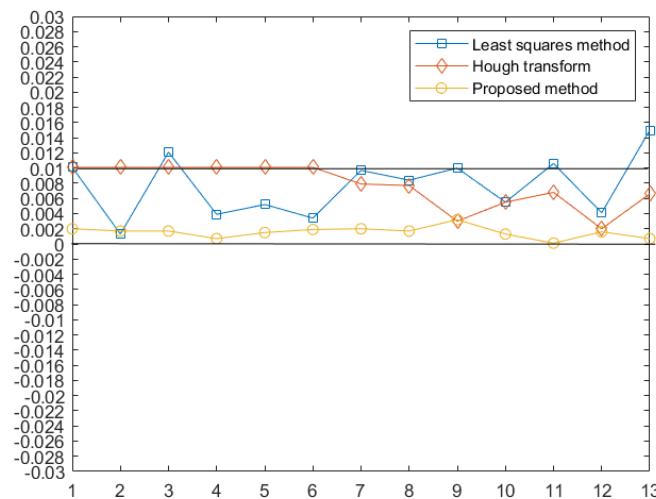


Figure 5. The diameter error curve of 145 type of punched steel strip.

To evaluate the accuracy of the fit, we used diameter absolute error, mean diameter deviation $AD(r)$ and diameter deviation variance $MSE(r)$ for fitted round holes and exact round holes.

$$AD(r) = \frac{2}{K} \sum_{i=1}^K |r_i - r| \tag{14}$$

$$MSE(r) = \frac{2}{K} \sum_{i=1}^K (r_i - r)^2 \tag{15}$$

In the above equation, r is the radius of the circular hole and r_i is the estimated circle radius. K is the number of round holes.

The measurement parameters of 145 type of nickel-plated punched steel stripe calculated by three different methods are given in Table 3.

Table 3. The measurement parameters of 145 type of punched steel strip.

Parameters	Average Hole Diameter (mm)	Diameter Absolute Error (mm)	Diameter Deviation Variance (mm)	Diameter Deviation Variance $MSE(r)$ (mm ²)	Running Time (s)
Standard value	1.963	<10 um	/	/	/
Proposed method	1.9615	0.0015	0.000029	0.0034	3.4375
Least squares method	1.9614	0.0016	0.000073	0.01655	3.3906
Hough transform	1.9571	0.0059	0.000066	0.0154	7.7154

As can be seen from Table 3, the diameter absolute errors calculated by the three methods are within the allowable range of 10 um. As can be seen from the above table, the proposed method has the lowest $AD(r)$ and $MSE(r)$, indicating the superiority of this method.

From the error curve of Figure 5, it can be seen that the diameter error of each circular hole calculated by the three methods varies greatly. However, the diameter error calculated by proposed method is within the allowable range to meet the requirements of the enterprise. In addition, it is not difficult to see that the least squares method has 5 error points that exceed the allowable range, while the Hough transform method has one more error point that exceeds the allowable range. From Table 3, it can be seen that the Hough transform takes the longest time, and the time of proposed method in this article is similar to that of the least squares method. Hence, considering the computational accuracy of the parameters and the real-time performance, this proposed method has better performance.

4. Conclusions

In this article, an improved circle fitting algorithm is proposed and implemented with the following innovations and advantages: (1) The algorithm in this article reduces the impact of noise points on the calculation, the complexity of the algorithm and the requirement of storage space by selecting different numbers of points for calculation several times, as well as improving the real-time performance of the algorithm. (2) The algorithm in this article uses the mean shift algorithm to obtain the optimal solution based on the results of multiple iterations of calculation, which makes the robustness of multi-circle detection significantly improved. Therefore, the algorithm in this article can be used in the multi-circle detection of industrial components with high requirements for real-time and operational accuracy.

Author Contributions: Conceptualization, B.C., J.L., Y.L., X.S. and W.L.; methodology, B.C., J.L., Y.L., X.S. and W.L.; software, B.C. and Y.L.; validation, B.C., Y.L., X.S. and W.L.; formal analysis, B.C., J.L., Y.L., X.S. and W.L.; investigation, B.C., J.L., Y.L., X.S. and W.L.; writing—original draft preparation, B.C., Y.L. and X.S.; writing—review and editing, B.C. and W.L.; visualization, J.L., Y.L. and W.L.; supervision, B.C. and J.L.; funding acquisition, B.C. and J.L. All authors have read and agreed to the published version of the manuscript.

Funding: This article was funded by the National Natural Science Foundation of China (grant no. 62273142), the Hunan Province Natural Science Foundation, China (Grant No. 2021JJ30477) and the science and technology innovation Program of Hunan Province (Grant No. 2021GK2010).

Conflicts of Interest: The authors declare no conflict of interest.

References

1. Li, C. A Study on Electrochemical Machining of Hole-Punched Steel Strip and Processes and Fundamentals of Nickel Electrodeposition. Ph.D. Thesis, Central South University, Changsha, China, 2013.
2. Tang, Y.; He, Y.; Zhong, J. A Kind of Perforated Steel Strip for Battery Plate. Chinese Patent CN 2715354Y, 3 August 2005.
3. Padilla, R.; Passos, W.L.; Dias, T.L.B.; Netto, S.L.; da Silva, E.A.B. A comparative analysis of object detection metrics with a companion open-source toolkit. *Electronics* **2021**, *10*, 279. [[CrossRef](#)]
4. Xin, M.; Wang, Y. Research on image classification model based on deep convolution neural network. *EURASIP J. Image Video Process.* **2019**, *2019*, 40. [[CrossRef](#)]
5. Huang, Z.; Yang, S.; Zhou, M.C.; Gong, Z.; Abusorrah, A.; Lin, C.; Huang, Z. Making accurate object detection at the edge: Review and new approach. *Artif. Intell. Rev.* **2022**, *55*, 2245–2274. [[CrossRef](#)]
6. Kvietkauskas, T.; Stefanovič, P. Influence of Training Parameters on Real-Time Similar Object Detection Using YOLOv5s. *Appl. Sci.* **2023**, *13*, 3761. [[CrossRef](#)]
7. Andriyanov, N.A.; Dementiev, V.E.; Tashlinskii, A.G. Detection of objects in the images: From likelihood relationships towards scalable and efficient neural networks. *Comput. Opt.* **2022**, *46*, 139–159. [[CrossRef](#)]
8. Malekjafarian, A.; Caprani, C.C.; Blacoe, S.; Guo, D.; Malekjafarian, A. Detection of vehicle wheels from images using a pseudo-wavelet filter for analysis of congested traffic. *IET Image Process.* **2018**, *12*, 12–20.
9. Djekoune, A.O.; Messaoudi, K.; Amara, K. Incremental circle hough transform: An improved method for circle detection. *Opt.—Int. J. Light Electron Opt.* **2017**, *133*, 17–31. [[CrossRef](#)]
10. Barbosa, W.O.; Vieira, A.W. On the improvement of multiple circles detection from images using hough transform. *TEMA* **2019**, *20*, 331–342. [[CrossRef](#)]
11. Gu, Y.; Lu, Y.; Yang, H.; Huo, J. Concentric circle detection method based on minimum enveloping circle and ellipse fitting. In Proceedings of the 2019 IEEE 10th International Conference on Software Engineering and Service Science (ICSESS), Beijing, China, 18–20 October 2019; pp. 523–527.
12. Lin, J.; Shi, Q. Circle Recognition Through a Point Hough Transformation. *Comput. Eng.* **2003**, *29*, 17–18.
13. Shakarji, C.M.; Srinivasan, V. On Algorithms and Heuristics for Constrained Least-Squares Fitting of Circles and Spheres to Support Standards. *J. Comput. Inf. Sci. Eng.* **2019**, *19*, 31011–31012. [[CrossRef](#)]
14. Zhang, J.; Chen, H.; Liu, F. Remote Sensing Image Fusion Based on Multivariate Empirical Mode Decomposition and Weighted Least Squares Filter. *Acta Photonica Sin.* **2019**, *48*, 199–210.
15. De Marco, T.; Cazzato, D.; Leo, M.; Distanto, C. Randomized circle detection with isophotes curvature analysis. *Pattern Recognit.* **2015**, *48*, 411–421. [[CrossRef](#)]
16. Comaniciu, D.; Meer, P. Mean shift: A Robust Approach Toward Feature Space Analysis. *IEEE Trans. Pattern Anal. Mach. Intell.* **2002**, *24*, 603–619. [[CrossRef](#)]
17. Yang, J.; Rahardja, S.; Frnti, P. Mean-shift outlier detection and filtering. *Pattern Recognit.* **2021**, *115*, 107874. [[CrossRef](#)]
18. Bahraini, T.; Azimpour, P.; Yazdi, H.S. Modified-mean-shift-based noisy label detection for hyperspectral image classification. *Comput. Geosci.* **2021**, *155*, 104843. [[CrossRef](#)]
19. Chaudhuri, D. A simple least squares method for fitting of ellipses and circles depends on border points of a two-tone image and their 3-D extensions. *Pattern Recognit. Lett.* **2010**, *31*, 818–829. [[CrossRef](#)]
20. Wei, T.; Liang, B. Iris location based on improved least square fitting. *Comput. Age Era.* **2016**, *6*, 75–79.
21. Yang, L.; Zeng, C.; Zhang, Y. An edge detection method for gray image based on mathematical morphology. *Foreign Electron. Meas. Technol.* **2012**, *31*, 27–30.

Disclaimer/Publisher’s Note: The statements, opinions and data contained in all publications are solely those of the individual author(s) and contributor(s) and not of MDPI and/or the editor(s). MDPI and/or the editor(s) disclaim responsibility for any injury to people or property resulting from any ideas, methods, instructions or products referred to in the content.